Atmos. Chem. Phys. Discuss., 11, 9165–9215, 2011
www.atmos-chem-phys-discuss.net/11/9165/2011/
doi:10.5194/acpd-11-9165-2011

Atmospheric Chemistry and Physics Discussions

Acetone variability in the upper troposphere: analysis of CARIBIC observations and LMDz-INCA chemistry-climate model simulations

T. Elias[1,*,], S. Szopa[1], A. Zahn[3], T. Schuck[2], C. Brenninkmeijer[2], D. Sprung[3], and F. Slemr[2]**

[1]Laboratoire des Sciences du Climat et de l'Environnement/CEA-CNRS-UVSQ-IPSL, UMR 8212, L'Orme des Merisiers, 91191 Gif-sur-Yvette, France
[2]Max-Planck-Institute for Chemistry Atmospheric Chemistry, J.-J.-Becher-Weg 27, 55128 Mainz, Germany
[3]Institute of Meteorology and Climate Research, Karlsruhe Institute of Technology, 76021 Karlsruhe, Germany
[*]now at: HYGEOS, Euratechnolgies, 165, Avenue de Bretagne, 59000 Lille, France
[**]now at: Honorary research associate at CRG, GAES, University of Witwatersrand, Johannesburg, South Africa

Received: 22 December 2010 – Accepted: 16 February 2011 – Published: 17 March 2011

Correspondence to: T. Elias (te@hygeos.com)

Published by Copernicus Publications on behalf of the European Geosciences Union.

ACPD
11, 9165–9215, 2011

Abstract

This paper investigates the acetone variability in the upper troposphere (UT) as sampled during the CARIBIC airborne experiment and simulated by the LMDz-INCA global chemistry climate model. The aim is to (1) describe spatial distribution and temporal variability of acetone; (2) define observation-based constraints to improve tropospheric modelling of the acetone; and (3) investigate the representativeness of the observational data set.

According to the model results, South Asia (including part of the Indian Ocean, all India, China, and Indochinese peninsula) and Europe are net source regions of acetone, where near 25% of North Hemispheric (NH) primary emissions and 40% of the NH chemical production of acetone take place. The impact of these net source regions on continental upper tropospheric acetone is studied by analysing CARIBIC observations of 2006 and 2007 when most flight routes stretch between Frankfurt, Germany, and Manila, Philippines, and by focussing over 3 sub-regions where acetone variability is strong: Europe-Mediterranean, Central South China and South China Sea. Acetone volume mixing ratio (vmr) in UT varies with the season, increasing from winter to summer by a factor 2 to 4. Spatial variability is also important, as acetone vmr may vary in summer by more than 1000 pptv within only 5 latitude-longitude degrees, and standard deviation on measurements acquired during a short flight sequence over a sub-region may reach 40%. 200 pptv difference may also be observed between successive inbound and outbound flights over the same sub-region, due to different flight specifications (trajectory in relation to plume, time for insulation).

A satisfactory agreement for the abundance of acetone is found between model results and observations, with e.g. only 30% over-estimation of the annual average over Central-South China and the South China Sea (between 450 and 600 pptv), and an under-estimation by less than 20% over Europe Mediterranean (around 800 pptv). Consequently, annual budget terms could be computed with LMDz-INCA, yielding a global atmospheric burden of 7.2 Tg acetone, and a 127 Tg yr^{-1} global source/sink strength.

ACPD

11, 9165–9215, 2011

Moreover the study shows that LMDz-INCA can reproduce the impact of summer convection over China when boundary layer compounds are lifted to cruise altitude of 10–11 km and higher. The consequent enhancement of acetone vmr during summer is reproduced by LMDz-INCA, to reach agreement on observed maximum of 970 ± 400 pptv (average during each flight sequence over the defined zone ± standard deviation). The summer enhancement of acetone is characterized by a high spatial and temporal heterogeneity, showing the necessity to increase the airborne measurement frequency over Central-South China and the South China Sea in August and September, when the annual maximum is expected (daily average model values reaching potentially 2000 pptv). In contrary the annual cycle in the UT over Europe-Mediterranean is not reproduced by LMDz-INCA, and in particular the observed summer enhancement of acetone to 1400 ± 400 pptv after long-range transport of free tropospheric air masses over North Atlantic Ocean. Confirmed agreement on the acetone annual cycle at surface level indicates misrepresentation of simulated transport of primary acetone or biased spatial distribution of acetone sinks and secondary sources.

1 Introduction

Hydroxyl radicals OH and HO_2 dominate background tropospheric chemistry through their oxidative capacity. As a matter of fact, the oxidation of CO and hydrocarbons is the main source of tropospheric ozone. Water vapour is the main precursor of primary tropospheric OH, except in the upper troposphere (UT) where dry conditions prevail. Here acetone (CH_3COCH_3) becomes a candidate as the main source of OH (Singh et al., 1995). Indeed, acetone was shown by Wennberg et al. (1998) to play a key role under specific conditions: considering 300 pptv acetone in a photochemical box model was sufficient to reach near agreement between measured and simulated OH concentration in the UT. The significance of acetone was confirmed using Chemistry-Climate Models: for example Folberth et al. (2006) showed with the LMDz-INCA model, that acetone and methanol play a significant role in the upper troposphere/lower stratosphere budget of

ACPD
11, 9165–9215, 2011

peroxy radicals, and an increase in HO_x concentrations of 10 to 15% was attributed to acetone. Chatfield et al. (1987) noted that acetone can be considered an indicator of properly modelled atmospheric chemistry in the UT, for instance as a tracer of previous photochemical activity in an air parcel.

It is currently accepted that the sources of acetone consist mostly of primary terrestrial biogenic and oceanic emissions, complemented by secondary chemical production, with sinks by photolysis and oxidation with a substantial degree of mostly dry deposition over land and oceans. Nevertheless, uncertainties remain in the acetone budget. For example, Jacob et al. (2002) improved the agreement between model and observational data by (1) adding an oceanic source, (2) increasing the terrestrial vegetation contribution, and (3) decreasing the contribution from vegetation decay. But in line with the fairly recent revision of the acetone photolysis quantum yield in terms of a temperature dependent function (Blitz et al., 2004), Arnold et al. (2005) estimated a reduced photolysis sink, that Marandino et al. (2006) proposed to compensate by increasing the ocean sink in order to accommodate results of air/sea flux measurements over the Pacific Ocean. Consequently, for total source/sink strength of around 100 $Tg\,yr^{-1}$, estimates of the oceanic contribution currently range between a net source of 13 $Tg\,yr^{-1}$ (Jacob et al., 2002) and a net sink of 33 $Tg\,yr^{-1}$ (Marandino et al., 2006). Concerning primary terrestrial biogenic emission, Potter et al. (2003) proposed a wide range of source strengths between 54 and 172 $Tg\,yr^{-1}$ for terrestrial vegetation and 7 and 22 $Tg\,yr^{-1}$ for plant decay.

Most recent budget studies relied on data compiled by Emmons et al. (2000): (1) the ocean source was taken into account for improving agreement over the Pacific Ocean (Jacob et al., 2002; Folberth et al., 2006); (2) the terrestrial biogenic primary emissions were modified to fit lower tropospheric observations (Jacob et al., 2002); (3) the acetone photolysis quantum yield (with its strong impact in the UT, Arnold et al., 2004) was changed to improve agreement for the vertical column (Arnold et al., 2005), especially over the Pacific Ocean. This all shows the problem of sorting out the budget of acetone, which by its variability adds an additional challenge. Because

ACPD
11, 9165–9215, 2011

measurements made onboard airplanes during field campaigns are essentially "snapshots", Emmons et al. (2000) claim that their data composite can not be regarded as climatology. Observation-based constraints need to be more complete to become applicable to all modelled source, sink and transport processes. In particular, few measurements were hitherto available in the northern mid-latitude UT and over continents, and temporal variability in the UT has been sounded sporadically only.

The approach of the CARIBIC experiment (Civil Aircraft for Regular Investigation of the atmosphere Based on an Instrument Container) (Brenninkmeijer et al., 2007) and other projects such as MOZAIC (e.g., Marenco et al., 1998; Thouret et al., 2006) and CONTRAIL (Machida et al., 2008) to use civil aircraft, provides an opportunity to more systematically sample the annual cycle and the inter-annual variability of main atmospheric trace gases on a large scale. CARIBIC, with its extensive equipment set is suitable to help to address the acetone budget problematic. Sprung and Zahn (2010) compiled three years of CARIBIC data to derive the acetone distribution around the tropopause north of 33° N, showing that acetone volume mixing ratio (vmr) varies by a factor 4 with season.

The purpose of this work is to scrutinize model results and observations for (1) describing spatial distribution and temporal variability of acetone vmr in the UT; (2) defining observation-based constraints to improve tropospheric modelling of the acetone field; and (3) investigating the representativeness of the observational data set. The simulation results are provided by LMDz-INCA, which integrates a comprehensive representation of the photochemistry of methane and volatile organic compounds from biogenic, anthropogenic, and biomass-burning sources (Folberth et al., 2006). The CARIBIC experiment provides the acetone measurements in the UT mainly over NH continental regions where major sources are located and where chemical activity significantly contributes to acetone sources and sinks. Main flight routes for the period considered are to Manila, Philippines, also providing the opportunity to study the impact of rapid uplifting of pollutants over China and South China Sea.

ACPD
11, 9165–9215, 2011

The LMDz-INCA model and the CARIBIC experiment are described in Sects. 2 and 3 respectively, together with the method used to compare the two data sets. Budget terms on global and regional scales are also provided in Sect. 2. Results are discussed in Sect. 4. Focus is on the UT over South-Central China and the South China Sea, with impacts of pollution events, and over the Europe-Mediterranean region affected by long-range transport over North Atlantic Ocean. Measurements of O_3 and CO are also used to discuss the chemical signature of air masses, with the help of computed back-trajectories.

2 Global budget of acetone according to LMDz-INCA

2.1 The LMDz-INCA set-up

LMDz-INCA consists of the INteraction Chemistry-Aerosols (INCA) module representing tropospheric chemistry, coupled with the Global Circulation Model LMDz (Hourdin et al., 2006). Fundamentals are presented by Hauglustaine et al. (2004) and first results with the full tropospheric chemistry are presented by Folberth et al. (2006). This model is commonly used in international multi-model experiments to investigate climate-chemistry issues or intercontinental transport (e.g. Sanderson et al., 2008; Fiore et al., 2009). Global tropospheric fields of greenhouse gases (CO_2, CH_4, O_3, ...), aerosols, water vapour and non-methane hydrocarbons are simulated on a horizontal grid being improved since Folberth et al. (2006), from 96×72 to 96×96 grid cells in the LMDz4-INCA3 version used here. Large scale advection is nudged using ECMWF reanalysis data. The number of reactive species in INCA has been increased from 83 (of which 58 are transported) to 89. Currently 43 photolytic, 217 thermochemical and 4 heterogeneous reactions are integrated in the INCA module. In particular, the acetone is directly involved in 21 reactions, e.g. in oxidation of alkenes, alkanes, alpha pinenes, and photolysis. The quantum yield for acetone photolysis is updated according to Blitz et al. (2004).

ACPD
11, 9165–9215, 2011

Primary biogenic emissions of isoprene, terpenes, methanol, and acetone are prepared by the global vegetation model ORCHIDEE (ORganizing Carbon and Hydrology In Dynamic EcosystEms) (Krinner et al., 2005), as described in Lathière et al. (2006). Primary emission of acetone by biomass burning is taken from van der Werf et al. (2006) (GFED-v2). The anthropogenic contribution is based on the EDGAR v3.2 emission database (Olivier and Berdowski, 2001), except for non-methane volatile organic compounds, which is based on the EDGAR v2.0 emission database (Olivier et al., 1996). The ocean source is derived from Jacob et al. (2002). GCM primitive equations are resolved by LMDz every 3 minutes, the large scale transport has a time step of 15 min, and physical processes of 30 min. INCA computes primary emissions, deposition and chemical equations every 30 min.

Folberth et al. (2006) compared volatile organic compounds fields simulated by the NMHC1.0 model version with field campaign results presented by Emmons et al. (2000) and Singh et al. (2001). Their simulated values have been sampled from the model output over the same regions and months as the airborne observational data: western North Atlantic Ocean in summer, eastern North Atlantic Ocean and tropical Atlantic Ocean in early autumn, East Asian coasts in winter, Pacific Ocean in early spring. Folberth et al. (2006) show a satisfactory overall agreement, with more frequent overestimation than underestimation. CARIBIC now allows to extend the available data set to continents and to investigate the seasonal variability (Sect. 3).

2.2 Budget terms

2.2.1 Global budget, sources and sinks

The budget terms computed with LMDz-INCA are presented in Table 1 together with literature results. Annual cycles of the global budget terms are shown in Fig. 1. Since no tendency is simulated for the annual global acetone burden, 2007 is used as reference for budget analyses. The global budget of acetone computed with LMDz-INCA shows identical total sink and source strengths of 127 $Tg\,yr^{-1}$, exceeding previous estimates. The total source in LMDz-INCA is apportioned as 60% primary terrestrial biogenic, 16%

ACPD
11, 9165–9215, 2011

primary oceanic, and 20% secondary chemical production. The biogenic contribution increased from 56 to 76 Tg yr^{-1} since Folberth et al. (2006), in close agreement with 66–71 Tg yr^{-1} presented by Lathière et al. (2006). This is at the lowest range estimated by Potter et al. (2003) of 61–194 Tg yr^{-1} for biogenic emission (terrestrial vegetation and plant decay). Consequently, primary emissions considered here are larger by 50% than used by Jacob et al. (2002), and by 25% relatively to Folberth et al. (2006) and Singh et al. (2004) (Table 1). In contrary, chemical production of 27 Tg yr^{-1} of acetone estimated by LMDz-INCA is similar to estimates by Jacob et al. (2002) (with 75% by C3-C5 alkanes according to Jacob et al., 2002 and Pozzer et al., 2010). The ocean source was kept constant at 20 Tg yr^{-1} following Folberth et al. (2006).

One third of the acetone load is deposited (mainly dry deposition), and two thirds is either oxidised or photolysed. Chemical destruction is similar to simulations by Jacob et al. (2002), but deposition computed by LMDz-INCA is increased to reach equilibrium of equal global source and sink strengths. The chemical budget by LMDz-INCA displays a net chemical sink of 53 Tg yr^{-1} on a global scale. The oceans are a net sink of 8 Tg yr^{-1}, resulting from 20 Tg yr^{-1} emissions and 28 Tg yr^{-1} deposition.

The mean residence time of 21 days is within the range inferred from previous studies (Table 1). However, like for the acetone source strength, our estimated atmospheric burden of 7.2 Tg is larger than previous estimates by Jacob et al. (2002), Arnold et al. (2005), and Marandino et al. (2006). A large simulated contrast exists between the NH and SH. With primary emissions being mostly located at the land surface, the total NH source strength is larger than in the SH. The budget is annually balanced over each hemisphere, with equal mean residence times of 21 days in each hemisphere. The annual mean NH atmospheric burden of 4.3 Tg is larger than in the SH. All sink and source strengths of the NH represent between 55 and 60% of the global terms with primary emission, chemical production, deposition and chemical loss of 55, 19, 27, 46 Tg yr^{-1} respectively. The net NH chemical sink is estimated to be 27 Tg yr^{-1}.

An exact balance between source and sink is not constantly found, causing a small seasonal variability of the global atmospheric burden of acetone. Annual cycles of the

ACPD
11, 9165–9215, 2011

global source and sink terms are shown in Fig. 1a. The signature of the dominant biogenic source causes maxima of the source terms to occur during boreal summer. Global primary emission increases by 1.6 from February to July–August and chemical production by 1.4. The NH annual cycle is stronger as primary production here more than doubles from February to July (not shown). Furthermore, primary emissions in the SH decrease from December–January to June. In February the primary emission is larger in the SH.

Because deposition and chemical loss depend on the atmospheric burden, on a global scale minima of the budget terms are found in boreal winter and maxima in boreal summer. Global deposition increases by a factor of 1.6, and chemical loss increases by 1.5. Chemical loss is always larger than deposition on a global scale. The global budget is annually balanced, but on a monthly basis, accumulation of acetone occurs in July at a rate of 0.7 Tg month^{-1}. Depletion occurs in December at a rate of −0.2 Tg month^{-1}. Taking into account the acetone residence time, the annual cycle of the atmospheric burden is delayed by 1–2 months, with a minimum of 6.4 Tg in February and a maximum of 8.1 Tg in September/October.

2.2.2 Regional features

Budget terms were also computed for NH continental regions including main route sections taken by the CARIBIC experiment in 2006–2007 (Sect. 3), namely South Asia and Europe (Table 2). The respective budget terms proportioned to those regions and monthly averages of the regional budget terms are plotted in Fig. 1b and c. Computations show that, on an annual basis, long-range transport tends to decrease the spatial heterogeneity in atmospheric burden caused by the high heterogeneity in source strengths, as a result of the sufficiently long residence time of acetone.

South Asia (Table 2) is a net source region, with 2 Tg yr^{-1} excess production, which is around 15% of the regional source strength of 13 Tg yr^{-1}. The excess of produced acetone is transported to other regions of the world, as on an annual basis, the acetone content (0.48 Tg acetone representing 11% of the NH burden) is proportional to

ACPD
11, 9165–9215, 2011

the covered surface area (11%). Regarding geographical extent, sources and sinks are proportionally more important over South Asia than on a hemisphere scale, with primary emission, deposition and chemical loss contributing around 15% of the NH terms. Moreover, with 4.8 Tg yr^{-1}, the chemical production represents 23% of the NH total. This excess in chemical production may account entirely for the excess production of acetone in South Asia. The net chemical sink is proportionally smaller than on a hemispheric scale, with 2.4 Tg yr^{-1} representing only 9% of the NH net chemical sink.

The annual cycles of the regional budget terms are similar to that of the global annual cycle in terms of seasonal minimum and maximum (Fig. 1b and c). Also the increases from winter to summer of chemical production and deposition are comparable. However the annual cycles have larger amplitudes: primary production increasing by a factor 2.3 and chemical loss by a factor 3. Primary production and chemical loss almost compensate, the excess production in the regions exhibits a weak annual cycle, with a minimum of 0.07 Tg $month^{-1}$ in September and a maximum of 0.29 Tg $month^{-1}$ in March. Finally, the atmospheric burden for South Asia varies between 0.37 Tg in April–May and 0.58 Tg in October.

As for South Asia, the atmospheric burden of acetone over the Europe-Mediterranean region (EurMed) is proportional to the surface area covered by the region (8% with 0.35 Tg acetone). The EurMed region also provides excess acetone during all seasons, which is likewise redistributed to other regions, varying from 0.1 Tg $month^{-1}$ in January to 0.2 Tg $month^{-1}$ in June and July (Fig. 1c), and cumulating to +1.7 Tg yr^{-1}, representing 25% of the regional source strength. Concomitantly, the annual chemical production is very important over EurMed, as it represents 33% of combined regional sources, while on a global scale chemical production represents 20% of combined sources. Of the NH chemical production 13% (9.3% global) occurs over EurMed (for 8% of the NH surface area), and even exceeds primary emission during the winter (Fig. 1c). This excess regional chemical production combined with a deficit simulated in regional chemical loss (accounting for only 6% of the NH chemical loss), almost results in net regional chemical balance. A strong seasonal variability is

ACPD
11, 9165–9215, 2011

simulated, namely from a net chemical sink of 0.2 Tg month^{-1} in summer, reversing to a net chemical source of 0.1 Tg month^{-1} in winter, while on a global scale there always is a net chemical sink. A large seasonal cycle is also simulated for primary production, varying from 0.1 Tg month^{-1} in January to 0.8 Tg month^{-1} in July. Deposition appears to be important over EurMed region as its magnitude is similar to chemical loss, and even exceeds chemical loss in winter, which is neither inferred for South Asia nor on a global scale. The annual cycle of the atmospheric burden over EurMed varies from 0.28 Tg acetone in March to 0.42 Tg in September.

Because primary emissions and dry deposition occur exclusively at surface level, the vertical profile of the global budget depends on the chemical terms only. Because the chemical budget results in a net sink on a global scale, the atmosphere is expected to be a sink for acetone. Consequently, lowest atmospheric layers are simulated to be net chemical source, with an overlaying net chemical sink, all along the year. Over Europe, the net acetone sink at 238 hPa can reach 500 Mg yr^{-1} and 100 Mg month^{-1} in August, and over South Asia it may reach 1500 Mg yr^{-1} and 200 Mg month^{-1} in August. Consequently, plumes of acetone at such altitude can only be observed thanks to transport of primary and secondary acetone from the boundary layer. The two net source regions Europe and South Asia will be discussed in Sect. 4, in terms of acetone content in the UT, as they are locations where most data is acquired by the CARIBIC experiment described in Sect. 3.

3 The strategy for comparing model data with CARIBIC measurements

3.1 CARIBIC data set

The CARIBIC project (http://www.caribic-atmospheric.com/) provides measurements of acetone volume mixing ratio (vmr) by an equipped airfreight container operated during regular long-distance flights of Lufthansa (Brenninkmeijer et al., 2007). Four consecutive intercontinental flights are made almost monthly, thus covering around

ACPD
11, 9165–9215, 2011

400 000 km annually. Acquisition is performed during all seasons, for a large range of solar insulation conditions, and along four main routes. In 2006 and 2007, most flights were to Manila, with two flights to South America (February and March 2006), and two to North America (September 2007). The measurement technique using a Proton-Transfer-Reaction quadrupole Mass Spectrometer was described by Sprung and Zahn (2010). The total uncertainty of the acetone data is ~10% above 200 pptv and ~20 pptv below 200 pptv. With a 1-min temporal resolution, approximately 10 000 values are available each year. The CARIBIC data set presented highly variable acetone values due to differences in sampled air masses (Köppe et al., 2009), pollution events (Lai et al., 2010), season, and aircraft localisation relatively to the tropopause (Sprung and Zahn, 2010). First we briefly summarise some key results from these studies.

Köppe et al. (2009) identified five air mass types using cluster analysis applied to a data set composed of mixing ratios of cloud water, water vapour, O_3, CO, acetone, acetonitrile, NO_y and of aerosol number densities, measured exclusively on flights to Guangzhou and Manila in 2006 and 2007. The cluster analysis could not be applied if one or more measured parameters were missing. Consequently, due to incidental instrument failure and calibration intervals, air mass characteristics could be identified for only one third of all acquisitions (Köppe et al., 2009). Five air mass clusters were defined for the summer and winter seasons, with Boundary Layer (BL), Free Troposphere (FT), Tropopause (TP) and Lowermost Stratosphere (LMS), common for summer and winter. The High Clouds (HC) cluster was defined exclusively for summer, which was replaced by a second FT cluster in winter. April data could neither be assigned to winter nor to summer.

In 2006 and 2007, TP was the most frequent air mass signature found in summer (31%), and FT was the most frequent one in winter (32 + 15%) (Köppe et al., 2009). Acetone vmr seems to be related with the air mass origin: e.g. acetone vmr in summer was 270 pptv (±65% standard deviation) in LMS and was 1230 pptv (±31%) in FT air masses (Köppe et al., 2009). In winter acetone vmr was overall almost half, in between

ACPD
11, 9165–9215, 2011

150 pptv (±50%) in the LMS and 700 pptv (±35%) in the BL. The seasonal change depended on the identified air mass: it was strong in FT air masses where acetone vmr decreased by a factor 2 or more from summer to winter. It was less important in BL, where acetone vmr decreased by only 30%. Largest CO vmr values were encountered in BL during winter and summer, with an averaged value of 100 ppbv (±20%) (Köppe et al., 2009). In the troposphere, largest mixing ratio of O_3 was encountered in summer FT, with averaged value of 130 ppbv (±30%), similar to both winter and summer TP (Köppe et al., 2009).

Sprung and Zahn (2010) discriminated tropospheric data from stratospheric data, and also defined a height above the tropopause. Data was acquired by CARIBIC mostly in the troposphere (76% in 2006, 64% in 2007) and in the stratosphere mainly for latitudes larger than 30° N, at pressure levels in the 200–250 hPa interval. The location of sampling relative to the tropopause was decisive as the averaged acetone vmr in 2006 was 530 ± 290 pptv in the upper troposphere and 350 ± 250 pptv in the stratosphere. Acetone decreased further down to 230 ± 150 pptv 0.5 km above the tropopause. Strong seasonality was observed north of 33° N, where a maximum of ~900 pptv was observed in summer and lowest values of ~200 pptv in winter at the tropopause (Sprung and Zahn, 2010). The air mass identification techniques by Köppe et al. (2009) and Sprung and Zahn (2010) are complementarily used in this paper.

The CARIBIC data set shows large spatial and temporal variability in acetone vmr measured in the upper troposphere in 2006 and 2007. This is illustrated in Fig. 2, which displays acetone vmr from several flights with values between 100 and 2600 pptv. The annual maximum acetone concentration in the UT was observed over Germany in July 2006 (flight #154), just after the ascent from Frankfurt airport: acetone varied between 1200 and 2600 pptv along 50° N latitude, from 15 to 22° E (Fig. 2) at a constant altitude of 280 hPa. The 2007 maximum was observed in August over eastern Kazakhstan during a flight from Guangzhou to Frankfurt (#205): acetone varied between 1000 and 2200 pptv along 50° latitude between 50 and 60° longitude, at 240 hPa. According to Moore et al. (2010), globally, maximal values in August 2003 were found to reach

ACPD
11, 9165–9215, 2011

3000 pptv between 300 and 500 hPa and to reach 2000 pptv above 200 hPa. Lai et al. (2010) showed the impact on acetone vmr of pollution events observed in the UT in April 2007. Polluted air masses crossing the flight trajectory over China led to enhancements from 350 to 1800 pptv for acetone, from 70 to 150 ppbv for CO with O_3 remaining below 100 ppbv. Back trajectories located the air mass origin over the Indochinese Peninsula, bringing pollution from biomass/biofuel burning activities (Lai et al., 2010).

3.2 Methodology to compare observed data to model results

In this paper, besides the 2006 and 2007 routes to Asia, routes to the Americas are used for comparison, thus extending the latitude that finally spans 30° S to 55° N. Model results are collocated to observations to allow comparison. Simulated values of acetone are spatially (vertically and horizontally) and temporally interpolated along the flight tracks, at the coordinates (time and space) of each data acquisition event.

To ensure consistency in the data set, small-scale variability due to changes in acquisition altitude are avoided by only using measurements when the aircraft cruises at constant altitude, i.e. when altitude difference between two successive acquisitions made in 1 min is smaller than 1 hPa. Consequently, the data set is mostly composed of measurements acquired at cruising altitudes above 300 hPa. Around 70% of the measurements were acquired at altitudes between 200 and 250 hPa and 25% at altitudes between 250 and 300 hPa. In rare cases such as over the South China Sea (in May and July 2006 (#151–152), in March and October 2007 (#184, #211–212)), data was acquired at lower altitudes between 400 and 600 hPa. Maximum altitude of acquisition was 177 hPa over continental South China (June 2006, August and October 2007).

Because the INCA module resolves only tropospheric chemistry, the height above the tropopause defined by Sprung and Zahn (2010) is used to remove measurements acquired in the stratosphere (in 2006, 25% of data acquisition in the stratosphere, and 35% in 2007). As measurement frequency in the stratosphere increases with latitude, most data acquired over northern Asia are screened out. The data set is then composed of 7500 observed values in 2006 and 6100 values in 2007. Most values

ACPD
11, 9165–9215, 2011

(around 60%) of acetone fall between 200 and 600 pptv. Consistently with Sprung and Zahn (2010), all air masses identified as LMS by Köppe et al. (2009) are localised in the stratosphere. Conversely, all summer HC and winter FT and BL cluster samples are localised in the troposphere. For 2006 and 2007, tropospheric air mass prints are identified for only 3400 data points. Moreover, as most flights started and finished in Frankfurt at night, measurements were chiefly made during the night (55% in 2007, 68% in 2006).

We define 11 geographical zones along all flight routes (Table 2) to compute regional averages of acetone vmr (one value per region and per flight), with the standard deviation as an indication of the spatial variability (the temporal variability of acetone is negligible in the few hours necessary to cross the zone). This approach is used for co-located simulation and measurement data sets. The annual cycle of acetone is illustrated by plotting time series of zonal averages (Fig. 5), which are analysed in the subsequent sections. During each round trip, given that the aircraft takes similar routes, it usually crosses in both directions a given zone twice within 24 h. Consequently, the time series for a year show commonly two points per month, reflecting daily variability.

We are also interested in examining the possible effects of irregularities in the CARIBIC sampling on properly representing the annual cycle. For that purpose co-located simulation and measurement averages are compared to averaged vmr simulated at constant altitude of 238 hPa, over the full zone for the whole month, referred to as climatological value thereafter, Also considered is how well spatial variability is represented by the standard deviations over all grid boxes of the different zones, as discussed in the subsequent sections.

ACPD
11, 9165–9215, 2011

4 Comparison of results

4.1 Effect of sampled air masses

Annual averages of measurements and co-located model results for each zone are presented in Table 2. It shows that the magnitude of acetone vmr in UT can be reproduced by LMDz-INCA, but disagreements occur as function of geography. Averaging the whole data set (7500 data points in 2006, and 6100 in 2007) provides a mean acetone value of 530 ± 290 pptv observed in the UT in 2006 and 640 ± 340 pptv in 2007. Bearing in mind the high standard deviation as a result of significant spatial and temporal variability of acetone along the flight tracks, there is a satisfying agreement with simulations. Acetone vmr generally appears to be larger over the continents than over the oceans. The largest observed averages are encountered over the EurMed region, being between 770 ± 520 pptv and 860 ± 500 pptv over the two years, having also the largest standard deviation. Smallest observed averages are found at around 400 pptv over the Tropical Atlantic Ocean in February and March 2006, with a standard deviation between 120 and 240 pptv, and also over South America but these values are representative of a unique season (boreal winter). Averages over the North Atlantic Ocean (NAO) give an indication of the seasonal impact: acetone doubles from winter 2006 to summer 2007. Average values over the South China Sea are also small, around 450 pptv in 2006 and 2007, but with large standard deviation (around 50%) due to measurements extending over several seasons.

LMDz-INCA usually over-estimates acetone, except over EurMed in 2006, over the NAO and over Eastern North America in 2007, and over Central Asia in 2007 (Table 2). Best agreement is found in northern Europe and northern Asia, where differences are smaller than 70 pptv in 2006 and 2007, for observed averages between 430 ± 220 pptv and 720 ± 280 pptv, respectively. The smallest simulated average is found over the NAO in winter 2006, providing a satisfying agreement with observation. Largest simulated values are not found over EurMed region, but rather over South America and the Tropical Atlantic Ocean, with averages between 900 and 1150 pptv, with largest

ACPD
11, 9165–9215, 2011

standard deviation between 500 and 900 pptv. Figure 2 (flight #141) shows indeed an extensive, dense plume simulated over tropical South America. The disagreement between observations and simulations is largest over South America and Tropical Atlantic Ocean, whereas agreement is satisfying in 2006 and 2007 over EurMed and CSChi.

Averages are also computed for the clusters identified by Köppe et al. (2009) in the winter and summer troposphere in 2006 and 2007, independent on the location along the flight track between Frankfurt and Manila. A scatterplot of simulations and measurements is provided in Fig. 3. Agreement between observation and modelling is satisfying for BL, HC and TP in summer 2007. However, the model underestimates strongly observations made in FT during summer in both 2006 and 2007. The 2007 maximum observed average is 1390 ± 310 pptv in FT, but simulation yields only 730 ± 100 pptv. For 2006 the maximum observed value is 1630 ± 330 pptv with only 780 ± 100 pptv from the simulation. The largest simulated value of 920 ± 270 pptv is for 2007 summer BL, providing good agreement with the observation of 1010 ± 240 pptv, which is second annual largest observed value. Observed 2006 summer BL is also second annual largest value with 980 ± 240 pptv, but in contrary to 2007, it is significantly underestimated by modelling. Smallest observed values in winter and summer correspond to TP air mass that may have experienced some stratospheric influence. They are over-estimated by modelling. In HC air masses, comparison results depend on the year. The simulations underestimate measurements in 2006 but overestimate them in 2007. Observations show seasonal dependence for BL and FT air masses in 2006 and 2007, which is fairly well reproduced in 2007: averaged acetone vmr is smaller than 700 pptv in winter 2007 and is larger than 700 pptv in summer 2007. Figure 3 clearly shows for 2006 a tendency to underestimate BL and FT in summer with in contrary a tendency to overestimate in winter.

Given the results of Fig. 3, and by studying the frequency occurrence of air masses over the different zones, we may gain insight by comparing results according to geographical location and season. In winter, satisfying agreement is found only for BL in 2006 and for FT-2 in 2007, for other air masses strong over-estimations are found.

ACPD
11, 9165–9215, 2011

With the 2006 winter BL and 2007 winter FT-2 being mostly encountered over CSChi, it is expected to find best agreement in winter over CSChi, and an over-estimation over other zones. Maximum acetone vmr being observed in summer FT air mass, the maximum observed over EurMed (Table 2) is explained by the high frequency occurrence of FT over EurMed in summer. Also, because a strong under-estimation is found in FT air masses, it is expected to significantly underestimate acetone vmr over EurMed in summer. Over-estimation in winter over EurMed together with an under-estimation in summer induces an averaged satisfactory agreement for EurMed in 2006 and 2007, as shown in Table 2. In contrary, FT is found in less than 10% of the cases over CSChi in 2006 and 2007, but in summer 2006 and 2007, HC is found in around 40% cases, TP in 33%, BL in 25%. Better agreement is therefore expected over CSChi than over EurMed in summer.

4.2 Focus on Europe-Mediterranean, Central-South China and South China Sea regions: acetone variability

We focus on flight sections included in the European and South Asian extended regions (last entries in Table 2) which both harbour net sources. According to LMDz-INCA 25% of the NH primary emissions and near 40% of the NH chemical production occurs here (Sect. 2). The regional atmospheric burden of acetone is proportional to the regional surface area (19%) on an annual basis, thanks to long-range transport on shorter time scales. As an example of modelled acetone transport in the UT, Fig. 2 shows that a plume observed over Central-South China (CSChi) during the July 2007 (flight #198) also covers North India and the Himalayas. The South Asia extended region (Table 2) is assumed to include the acetone plume thus impacting the acetone burden over CSChi and South China Sea (SCSea). Moreover this region and the other extended Europe region (Table 2) are the two regions most intensively sampled by CARIBIC during the Frankfurt – Manila flights 2006 and 2007. Indeed flights crossed 18 times EurMed in the troposphere, and Central-South China around 30 times (Table 2). The CARIBIC experiment thus allows studying the impact of acetone emission and

ACPD
11, 9165–9215, 2011

transport on its spatial distribution in the UT over the Eurasian continent, as well as its seasonal variability.

Scatterplots of 2006 and 2007 flight averages of co-located simulations and measurements are plotted in Fig. 4a, b and c for CSChi, SCSea and EurMed, respectively (Table 2). The flight average is the average of measured acetone vmr during the flight leg contained in the defined zone. Modelling reproduces the variability of acetone vmr in the UT over CSChi (Fig. 4a) fairly well with only 30% mean overestimation by LMDz-INCA. The flight averages of measured acetone vary by a factor 2 in 2006 and by a factor 3 in 2007, while flight averages of simulated acetone vary by a factor of around 2.5 in 2006 and 2007. Moreover measurement and simulation also agree concerning the standard deviation which can reach 400 pptv or 40% of the flight average (for measurements and simulation of e.g. October 2006). Agreement is particularly satisfying for acetone vmr observed in excess of 800 pptv. All points fall between 100% agreement and the factor-2 overestimation line, except for 6 outliers (e.g. model overestimation of 2006 and 2007 minima on flights #177 and #178 in winter (Fig. 2)).

Overall variability is also reproduced by modelling over SCSea (Fig. 4b), where the flight average of acetone vmr varies by a factor of 2 to 4 in 2006 and 2007 according to observation, and by a factor of around 2 according to modelling. Agreement is particularly satisfactory for observed maxima of 670 ± 100 pptv in 2006 and 870 ± 150 pptv in 2007 (flights #152 and #199). In contrary, observed minima of 210 ± 50 pptv are strongly overestimated in 2006 and 2007 (flights #172 and #183). As for CSChi, we can note an overall slight overestimation.

Finally (Fig. 4c) LMDz-INCA reproduces the magnitude of acetone vmr over EurMed but not its temporal variability. The observations indicate large variability of averaged acetone vmr as well as large standard deviations. Acetone vmr varies from less than 500 pptv to around 1500 pptv (except for the minimum of 120 pptv measured over North Africa during flight #141, returning from Sao Paulo (Fig. 2)). Summer observed maximum is consistent with retrievals from MIPAS-E (Moore et al., 2010) sounding the upper troposphere in August 2003: daily averages vary between 1200 and 1600 pptv

ACPD
11, 9165–9215, 2011

between 45° N and 90° N at 277 hPa. The standard deviation can reach values as high as 700 pptv for the 2006 maximum observed on 5 July 2006 (flight #154). However modelling provides little variability, with averaged acetone vmr falling between 560 ± 50 and 930 ± 160 pptv in 2006 and 2007 (except for the minimum of 270 ± 10 pptv corresponding to the minimum observed over North Africa). Consequently, small observed acetone burdens over EurMed are overestimated whereas large burdens are underestimated, with agreement only being satisfactory for measured median values of around 750 pptv in spring.

4.3 Annual cycle in the UT over Europe-Mediterranean, Central-South China and South China Sea

Sprung and Zahn (2010) discussed the annual cycle of acetone vmr in the stratosphere and at the tropopause over the Eurasian continent north of 33° N, based on their 2006 and 2007 data. Annual cycle is observed, with minimum acetone vmr of 200 pptv in midwinter at the tropopause and maximum of 900 pptv in summer. High standard deviation reaching 60% for the June maximum of 1000 pptv indicates that not only season affects acetone vmr, but also stratospheric influence and geographical heterogeneity (latitude varying from 10° E to 100° E). We focus on the troposphere and distinguish measurements in function of geography to reduce standard deviation. In 2006 and 2007, the CARIBIC aircraft route crossed the EurMed, CSChi and SCSea tropospheric regions almost every month (Table 2), providing the opportunity to study the geographical variation of the annual cycle of acetone vmr in UT. The time series of flight averages of co-located simulations and measurements plotted in Fig. 5 show that most of the variability observed for CSChi and SCSea (Fig. 4a and b) is due to the seasonal variation which is well reproduced by the model.

The annual CSChi maximum of 970 ± 400 pptv in 2006 is observed in October and the maximum of 960 ± 300 pptv in 2007 is observed in July when also the standard deviation is largest (Fig. 5a–b). The 2006 and 2007 minima of 300 ± 60 and 150 ± 50 pptv, respectively, are observed in winter, when also the variability is at its minimum. The

ACPD
11, 9165–9215, 2011

observed increase of acetone vmr from winter to summer is reproduced by modelling, as averaged co-located simulations for 2007 show a minimum in winter and a maximum in July. In 2006, the minimum observed in December is overestimated, but the minimum simulation of 440 ± 100 pptv for May (no measurements made earlier) reproduces the observation.

Seasonal variation is as intense over the South China Sea (Fig. 5c–d) as over Central-South China. An annual maximum of 670 ± 100 pptv is observed in May 2006 and of 870 ± 150 pptv in July 2007 (same day as over CSChi), with a minimum of 210 ± 50 pptv in November 2006 and in March 2007. Agreement between model results and data is found in August 2007 over both SCSea and CSChi (#205 flight back to Frankfurt, case study by Lai et al., 2010), however, strong over estimation occurs in autumn-winter 2006–2007. In October 2006, agreement is found over CSChi but not over SCSea because the observed plume is indeed simulated but not at the correct location (flight #168–169 Fig. 2). While it is observed North West of the CSChi zone, extending to Central Asia, it is simulated in the South East corner of the CSChi zone, also covering the entire SCSea zone. Therefore, even if the location is not reproduced, agreement is still found for average and standard deviation over CSChi, however, the over-estimation is significant over SCSea.

Finally, according to observation, acetone exhibits a strong annual cycle over EurMed (Fig. 5e–f). Flight averages as well as standard deviations increase significantly in June, July and August 2006 and 2007, reaching larger values than over SCSea and CSChi, and minimum is observed in February 2006 and 2007, while, as discussed in the Sect. 4.2, modelling fails to simulate an annual cycle over EurMed.

4.4 Was the CARIBIC flight frequency sufficient to assess a climatological annual cycle of acetone?

Given the agreement between simulation and measurement in the UT over CSChi, modelling can be used to assess the effect of incomplete or sparse airborne sampling on the representativity of the annual cycle. The climatological annual cycle is plotted

ACPD
11, 9165–9215, 2011

in Fig. 5 together with both the measured and simulated sampled annual cycle. The disagreement between the two approaches to represent the annual cycle shows the limitation of airborne sampling when acetone burdens are highly variable, as occurs in summer. The annual cycle sampled over CSChi agrees with the climatological cycle (Fig. 5a–b): the minimum of below 500 pptv, together with the minimum standard deviation both occur in winter; acetone vmr increases in both magnitude and standard deviation towards summer. However, according to the monthly climatological average, the maximum should occur in September (2006 and 2007) with monthly averaged acetone vmr of around 1100 pptv, and not in July, as observed in 2007, nor in October as observed in 2006. No measurements were made over CSChi in September 2006 and 2007 to check this simulated annual maximum. Moreover measurements made in August 2007 suggest that acquisition frequency (once per month) in summer might not be sufficient to catch the maximum. Indeed observation and modelling agree, indicating that the acetone vmr at the time of aircraft crossing was smaller than the climatological monthly mean by more than 200 pptv (Fig. 5b). For winter, the climatological annual cycle provides confirmation that the acetone vmr is always over-estimated, with nevertheless agreement on a small standard deviation.

According to modelling, the South China Sea region is more homogeneous than CSChi (except for May–June), as the climatological standard deviation remains small, in particular during the maximum in summer. The climatological annual cycle also confirms over-estimation in autumn-winter in UT over SCSea. In June and July, observations show important inter-annual differences between 2006 and 2007, but which is not simulated. In contrary, modelling and observation agree to indicate that the acetone vmr is close to 500–600 pptv in April–May. Surprisingly, the standard deviation of co-located simulations is large in March 2007 (flight #184) over SCSea, in contrary to measured standard deviation and to climatological standard deviation. This is because the aircraft flew at an occasional low altitude and that a strong gradient is simulated: simulation of 1400 pptv at 575 hPa, with observation of around 400 pptv. This does not affect the climatological values which are defined at constant altitude of 238 hPa.

ACPD
11, 9165–9215, 2011

4.5 Acetone enhancement in the summer monsoon plume in the UT: horizontal heterogeneity and daily variability of acetone vmr

Mean acetone vmr increasing from winter to summer, accompanied by increasing temporal and spatial heterogeneity, are indicative of an acetone plume. Daily simulations at 238 hPa corresponding to the flight #198 (July 2007) (Fig. 2) show that the daily averaged acetone vmr is larger than 1000 pptv for a large zone covering North India, the Himalayas to the Chinese Sea, consistent with the extended South Asian region defined for the budget computation (Sect. 2). In accordance with the annual cycle over CSChi, daily average of simulated acetone over the extended South Asian region increases from 400 to 1000 pptv from winter to summer, with the standard deviation increasing from 100 to 400 pptv (Fig. 6). The standard deviation increases because daily maxima increase from less than 1000 pptv in January–March to 3000 pptv in September, while the daily minimum remains relatively constant between 300 pptv in March and 500 pptv in November. The area covered by the acetone plume also increases from winter to summer, to cover half the South Asian region. Fig. 6 also shows that day-to-day variability can be very important, as the sudden decrease of more than 1000 pptv in few days after September.

Moreover, observation shows that the acetone variability within a single day can be large. Indeed, over CSChi, the time lag between inbound and outbound flights is generally between 10 and 17 h, while over SCSea it is smaller than 8 hours. This in-out shift can mean 240 pptv difference, as for August 2006 over SCSea and for August 2007 over CSChi (Fig. 5). Hourly shifts can be large even when modelling indicates a homogeneous acetone field. Examples are the 200 pptv change in February 2007 over CSChi and in October 2007 over SCSea. The in-out shift may be due to temporal variability or altitude differences, as the outbound flights over SCSea are generally higher by 20 hPa than the inbound flights, but lower than inbound flights over CSChi by more than 70 hPa. The change of acetone vmr with altitude is not systematic. The acetone vmr is sometimes observed to decrease with increasing altitude, as in August

ACPD
11, 9165–9215, 2011

and November 2006 over SCSea, and sometimes observed to increase with increasing altitude as in May 2007. Over CSChi, the acetone vmr decreases with increasing altitude in April and November 2006, and in February, June and August 2007, but remains constant despite altitude change in May and October 2007.

4.6 Effects of vertical gradients

Section 4.5 suggests that vertical gradients of acetone vmrs might affect flight based averages significantly. Modelling indeed shows that acetone vmrs vary with altitude. Simulated monthly vertical profiles are plotted in Fig. 7, for 2 cases: (1) background conditions defined by acetone vmr at 238 hPa being below 1000 pptv, (2) "ppbv-event" conditions defined by acetone vmr at 238 hPa larger than 1000 ppbv. During background conditions, the acetone vmr continuously decreases with altitude. In contrary, during the ppbv-event, a local minimum is simulated between 400 and 600 hPa, indicating an acetone plume located above (except for September, when the plume seems to extend down to the surface as acetone vmrs remain higher than 1300 pptv below 238 hPa). Largest values at surface level are reached during the 238-hPa ppbv-event. From May to November, the acetone vmr is above 2500 pptv, and even reaches 3400 pptv in July, while under background conditions acetone vmr is between 1600 and 2200 pptv at surface level. However, during early spring, acetone vmrs at the surface can be smaller than acetone vmr at 238 hPa, and even smaller than in background conditions. Simulation of the acetone plume location is consistent with simulations by Park et al. (2004) of a plume composed of high mixing ratios of CH_4, H_2O and NO_x at pressure altitudes included between 300 and 150 hPa, in accordance with observations from the HALOE instrument. The observed monsoon plume in CH_4 is also reported by the AIRS instrument to be situated in the altitude interval from 300 hPa to 150 hPa (Xiong et al., 2009).

While modelling over EurMed does not reproduce the observed variability of acetone in the UT, it does provide variability at surface level. Simulated vertical profiles over Europe (not shown) are similar to vertical profiles over South Asia, but under background conditions, indicating no ppbv-event is observed at 238 hPa. The averaged

ACPD
11, 9165–9215, 2011

acetone vmr varies between 500 and 700 pptv at 238 hPa and between 1300 and 2200 pptv at surface level. Such variability at surface level is correlated with season change. Comparisons are made with ground-based observation presented by Solberg et al. (1996) and already used by e.g. Jacob et al. (2002) and Folberth et al. (2006). Time series of monthly averages of acetone vmr are plotted for 6 European sites in Fig. 8. Similarly to the observations in the UT, an annual cycle is observed at the surface sites, but it is highly dependent on location. The timing and magnitude of the maxima varies: the maximum is observed from May in Birkenes to August in Donon, between 1000 pptv in Rucova and 2000 pptv in Donon. The minimum is observed between 300 pptv in Birkenes and 600 pptv in Waldhof. In contrary to the UT, the model is able to simulate an intense annual cycle at surface level, with acetone vmr increasing by a factor 2.5 from winter to summer. Except in Birkenes where the maximum is simulated in June (agreeing with observation), the maximum is simulated in August–September, somewhat later than observed. Agreement between modelling and observation is satisfying in spring-summer at 48–49° N sites, from March to July in Kosetice and to August in Donon. The maximum magnitude is reproduced, but the minimum is overestimated, as it is the case in the UT over Central-South China and South China Sea. In contrary, the minimum in Waldhof in January–March is reproduced by modelling. For the 56–58° N sites of Birkenes and Rucova, modelling constantly overestimates the observations by 500 to 1000 pptv.

Systematic overestimation in autumn (for all sites) is similar to Jacob et al. (2002) a priori modelling, which was attributed to an overestimated emission from plant decay as an acetone source peaking in September–October. Jacob et al. (2002) then proposed reducing the global plant decay contribution to fit measured annual cycles. A shift to autumn in the annual cycle has also been simulated for another oxygenated specie, methanol, and with the same LMDz-INCA model, in the 60–90° N latitude (Dufour et al., 2007). The authors attribute long residence time responsible to the accumulation of methanol. Thus reducing land deposition in autumn and winter might improve agreement with observation for methanol, but it could also be envisaged for acetone.

ACPD
11, 9165–9215, 2011

4.7 Two contrasted transport conditions: rapid uplifting of pollutants over Central-South China and long-range transport to Europe-Mediterranean region

We have described how acetone vmrs are under-estimated in summer FT air masses encountered over Europe-Mediterranean region, and, in contrary, better agreement is found in summer BL and HC air masses sampled over Central-South China. We discuss here the impact of different transport conditions, which implies different chemical activity in the transported air masses, witnessed by a different relation between acetone content and CO and O_3 contents.

Five-day back-trajectories are computed based on meteorological analysis data from the European Centre for Medium range Weather Forecasts (ECMWF) (van Velthoven, 2009), with the KNMI trajectory model TRAJKS (Scheele et al., 1996) for every 3 min of flight. Back-trajectories plotted in Fig. 9 are computed for plumes observed in July 2006 and 2007 (flights #154 and #198). Two plumes are observed during flight #154 (Fig. 2), with acetone vmr in excess of 2000 pptv around 21:40 GMT 5 July 2006, and in excess of 1000 pptv around 05:20 GMT 6 July 2006. Three plumes are observed during flight #198 (Fig. 2), with acetone vmr in excess of 1500 pptv around 22:10 GMT 17 July 2007, in excess of 1000 pptv around 04:10 GMT 18 July 2007, and in excess of 1500 pptv around 06:20 GMT. The European plume, assigned with FT air mass print in July 2007 (no air mass assigned in July 2006), originates from long-range transport from North America or the North Atlantic Ocean. The North Chinese plume, with mainly HC and few BL signatures, originates from the local boundary layer with only few days of travel time (Fig. 9d), and the South Chinese plume, with BL signature, originates from regional transport from India (Fig. 9e).

The transport conditions over China are similar to the impact of the summer monsoon observed over India, which was subject of many publications. The summer monsoon affects the composition of the UT by dynamical and meteorological processes, basically strong and rapid convection lifting of boundary layer compounds combined with

ACPD
11, 9165–9215, 2011

high precipitation affecting emissions from certain sources. Consistent enhancements of CO, H_2O, CH_4, N_2O and non-methane hydrocarbons were observed with CARIBIC over South Asia in summer 2008 (Schuck et al., 2010; Baker et al., 2010). A concomitant decrease of ozone was also observed by CARIBIC (Schuck et al., 2010). Model and satellite data consistently localised high mixing ratios of CH_4 between 60° E and 120° E around 30° N, a region included in our extended South Asian region (Table 2). The enhancements were at pressure altitudes between 300 and 100 hPa (Park et al., 2004; Xiong et al., 2009), at and above cruising altitude. Schuck et al. (2010) showed that air masses sampled north of 30° N generally travel for more than a week, in contrast with air masses south of 30° N which had ground contact within the last four days prior to sampling. Baker et al. (2010) confirmed that in the southern monsoon region, sampled air masses travelled 3 to 6 days before sampling, and 9 to 12 days in northern monsoon region. This is consistent with the summer BL air mass print mostly encountered over CSChi and SCSea (in 2006 and 2007), but rarely encountered over Northern Asia.

The CARIBIC data set shows that air masses sampled over EurMed and CSChi bear different chemical signatures. The chemical signature is deduced from the CARIBIC measurements of O_3 and CO vmrs. Values of CO larger than 140 ppbv occur only over CSChi and SCSea in 2006, and not over other regions. A maximum of CO vmr of 260 ppbv is measured over CSChi in July and August 2006 (for acetone vmr around 1700 pptv). Over EurMed, CO vmr is never observed larger than 120 ppbv.

CO vmrs increase with acetone vmrs. Most frequent values of CO vmrs measured over CSChi and SCSea are between 60 and 100 ppbv, while most frequent values lie between 80 and 160 ppbv when the acetone vmr is larger than 1000 pptv. The slope of acetone versus CO can be used to identify the sampled air mass (de Reus et al., 2003). Linear regressions with high correlation coefficient are plotted in Fig. 10, for HC, FT, and BL air masses sampled in 2006 and 2007 summers, when acetone vmr can increase (acetone vmrs are always smaller than 800 pptv in summer TP, while in summer BL 85% exceed 800 pptv, and in summer HC 30% exceeds 800 pptv). The

ACPD
11, 9165–9215, 2011

slope depends on the air mass type but might also depend on location. In particular for BL and HC air masses, the slope is steeper over EurMed and Central Asia (around 25 pptv acetone/ppbv CO) than over CSChi (around 6 pptv acetone/ppbv CO). For all summer FT air masses, the slopes are computed rejecting outliers with CO vmrs larger than 120 ppbv. The FT slope seems closer to the BL and HC slopes over EurMed and Central Asia (around 16 pptv acetone/ppbv CO).

Major contrast was found in chemical composition of the upper troposphere over East Mediterranean, between air mass origin over North Atlantic/North America (farther west than 0°) and over South Asia (farther east than 40° E) (Scheeren et al., 2003). CO vmrs are larger in South Asian air masses than in North Atlantic/North America air masses, while in contrary O_3 vmrs are smaller. Similar behaviour is observed in relation to our classification per region and per air mass print. Enhancement of both gases never occurs simultaneously, CO vmrs increase only in HC and BL air masses sampled over CSChi, with O_3 remaining smaller than 100 ppbv, and O_3 vmrs can increase in FT air masses and in HC and BL air masses over EurMed, but with CO vmr remaining smaller than 130 ppbv.

5 Conclusions

The purpose of this work is to: (1) describe spatial distribution and temporal variability of acetone vmr in the UT; (2) define observation-based constraints to improve tropospheric modelling of the acetone field; and (3) investigate the representativeness of the observational data set. Simulation results are provided by LMDz-INCA, a global chemistry climate model including the oxidation of methane and volatile organic compounds. The CARIBIC experiment provides the acetone measurements in the upper troposphere (UT) mainly over Northern Hemisphere continental regions where major sources are located and where chemical activity significantly contributes to acetone sources and sinks. Acetone is a key factor in UT chemistry, as a potential source of hydroxyl radicals, which are important components of the ozone cycle.

ACPD
11, 9165–9215, 2011

The regularity of the CARIBIC measurements (monthly flights) provides insight on seasonal variability of the acetone content. Measurements were made during intercontinental flights allowing exploring the influence of different air mass history, long-range transport in the free troposphere, rapid convective uplifting of boundary layer compounds, as well as land/sea contrasts. Consecutive inbound and outbound flights separated by a short stopover on almost identical routes also allow defining the sensitivity of the chosen flight track in relation to plume transport. Strong variability is observed. Acetone vmr in UT varies with the season by a factor 2 to 4, over Europe-Mediterranean and over Central South China. Spatial variability is also important, as acetone vmr may vary in summer by more than 1000 pptv within 5 latitude-longitude degrees, standard deviation reaching 40% of average over a defined zone. 200 pptv difference may also be observed between the inbound and outbound flights, due to different altitude of few tens hPa, different insulation conditions, or plume transport in relation to the flight track. The capacity of the LMDz-INCA Chemistry-Climate Model to reproduce all these features is assessed using two years of data.

A satisfactory agreement for the abundance of acetone is found between model results and observations, with 30% over-estimation of the annual average over Central-South China and the South China Sea, and an under-estimation by less than 20% over Europe Mediterranean. Consequently budget terms are computed. The mean annual atmospheric burden of acetone is 7.2 Tg, larger than previous estimates by several authors and even increased since last version of the LMDz-INCA model, because of enhanced primary emissions. The oceans contribute 20 Tg yr^{-1} to primary emissions, similar to the Jacob et al. (2002) estimate, and terrestrial biogenic emissions contribute 75 Tg yr^{-1}, consistent with the range proposed by Potter et al. (2003). In situ chemical production of acetone amounts to 27 Tg yr^{-1}, unchanged since Jacob et al. (2002). We focused the budget term analysis on two regions substantially sounded by the CARIBIC experiment. The South Asian and European regions are identified by the model simulation as important acetone sources regions on a global scale, providing respectively 2 Tg yr^{-1} and 1.7 Tg yr^{-1} excess produced acetone in relation to sinks.

ACPD
11, 9165–9215, 2011

This is essentially due to strong secondary chemical production of acetone reaching respectively 25% and 15% of the Northern Hemisphere chemical production.

The quality of the model results depends on geography and season. LMDz-INCA can reproduce magnitude of acetone vmrs in the UT over the North Atlantic Ocean, Europe-Mediterranean, North Europe, North Asia, Central Asia and Central-South China, but strong overestimation occurs over South America in February-March. However, air mass classification reveals systematic and significant under-estimation of acetone vmrs sampled in air masses with summer free troposphere (FT) signature, which witnesses largest observed acetone loads. In contrast over-estimation occurs in all winter air masses as well as in air masses with summer tropopause signatures. The second largest acetone load is observed in air masses with boundary layer print (BL), where agreement is good in 2007 but overestimation occurs in 2006. The FT signature is typical of long-range transport above the North Atlantic Ocean and North America to Europe, while BL air mass signature observed in the UT displays rapid convective uplifting of boundary layer compounds, similarly to the Asian summer monsoon condition. Consequently, the annual cycle can be captured by LMDz-INCA in UT over Central-South China, with acetone vmr increasing from winter to summer by a factor 2 to 3, despite an overall overestimation by around 30%, and no seasonal variability is reproduced in UT over Europe-Mediterranean region.

Based on the satisfying agreement over Central-South China, sampled information is extrapolated using LMDz-INCA. We show that monthly frequency of data acquisition might be too coarse for providing the annual cycle of acetone vmr with accuracy, as a plume structure is responsible for the acetone vmr increase, which presents strong spatial and temporal variability. For example during the August 2007 flight, the acetone vmr over Central-South China was 30% smaller than the monthly average, and a further 20% shift was observed between the inbound and outbound flights. In particular, missing measurements in September in both years prevents to check the simulated magnitude of the maximum, which can reach 3000 pptv as daily average at 238 hPa. In accordance with previous studies, LMDz-INCA shows that the plume is

ACPD
11, 9165–9215, 2011

located between 150 and 400–600 hPa, where data acquisition by long-distance aircraft is most frequent.

We checked with ground-based observation that the missing acetone plume over Europe is not typical of the whole column. LMDz-INCA displays seasonal variability of acetone at surface level, reaching agreement for spring-summer at some surface sites. Systematic over-estimation during autumn could be due to local sinks not simulated sufficiently strong. Over-estimation in winter seems systematic at surface level at European sites and also in the UT over Europe-Mediterranean, Central-South China, and South Chinese Sea.

Missing transport of primary emission up to the FT air masses might explain the discrepancy in UT over Europe-Mediterranean. Another explanation can be missing secondary acetone in FT air masses, due to incorrect global distribution of the chemical production source. The only sink in FT air masses is chemical destruction which could be over-estimated due to once again incorrect global distribution. Increasing global amount of acetone chemical production or decreasing global amount of chemical destruction are not recommended, as that would also impact acetone vmr over Central-South China, where over estimation is already observed. Observation constraints in UT over Europe-Mediterranean are 1400 ± 400 pptv in June-July-August and 300 ± 60 pptv in February (zonal average per flight). Summer flights to North America could provide insight on chemical activity in free tropospheric air masses transported to Europe.

The study underlines the need of metadata accompanying the observations such as air mass origin by cluster analysis and trajectory calculations. Furthermore it shows that the averaging of data in order to provide climatology is difficult to envisage due to the huge variability of such a species and thus should be handled carefully to validate satellite or global model results.

ACPD
11, 9165–9215, 2011

Acknowledgements. We acknowledge the support of the European Commission through the GEOmon (Global Earth Observation and Monitoring) Integrated Project under the 6th Framework Program (contract number FP6-2005-Global-4-036677). T. Elias was entirely funded by the GEOmon project. We gratefully acknowledge the support from all CARIBIC partners.

The publication of this article is financed by CNRS-INSU.

References

Arnold, S. R., Chipperfield, M. P., Blitz, M. A., Heard, D. E., and Pilling, M. J.: Photodissociation of acetone: Atmospheric implications of temperature dependent quantum yields, Geophys. Res. Lett., 31, L07110, doi:10.1029/2003GL019099, 2004.

Arnold, S. R., Chipperfield, M. P., and Blitz, M.: A three dimensional model study of the effect of new temperature dependent quantum yields for acetone photolysis, J. Geophys. Res., 110, D22305, doi:10.1029/2005JD005998, 2005.

Baker, A. K., Schuck, T. J., Slemr, F., van Velthoven, P., Zahn, A., and Brenninkmeijer, C. A. M.: Characterization of non-methane hydrocarbons in Asian summer monsoon outflow observed by the CARIBIC aircraft, Atmos. Chem. Phys., 11, 503–518, doi:10.5194/acp-11-503-2011, 2011.

Blitz, M. A., Heard, D. E., and Pilling, M. J.: Pressure and temperature-dependent quantum yields for the photodissociation of acetone between 279 and 327.5 nm, Geophys. Res. Lett., 31, L06111, doi:10.1029/2003GL018793, 2004.

Brenninkmeijer, C. A. M., Crutzen, P., Boumard, F., Dauer, T., Dix, B., Ebinghaus, R., Filippi, D., Fischer, H., Franke, H., Frie, U., Heintzenberg, J., Helleis, F., Hermann, M., Kock, H. H., Koeppel, C., Lelieveld, J., Leuenberger, M., Martinsson, B. G., Miemczyk, S., Moret, H. P., Nguyen, H. N., Nyfeler, P., Oram, D., O'Sullivan, D., Penkett, S., Platt, U., Pupek, M.,

ACPD
11, 9165–9215, 2011

Ramonet, M., Randa, B., Reichelt, M., Rhee, T. S., Rohwer, J., Rosenfeld, K., Scharffe, D., Schlager, H., Schumann, U., Slemr, F., Sprung, D., Stock, P., Thaler, R., Valentino, F., van Velthoven, P., Waibel, A., Wandel, A., Waschitschek, K., Wiedensohler, A., Xueref-Remy, I., Zahn, A., Zech, U., and Ziereis, H.: Civil Aircraft for the regular investigation of the atmosphere based on an instrumented container: The new CARIBIC system, Atmos. Chem. Phys., 7, 4953–4976, doi:10.5194/acp-7-4953-2007, 2007.

Chatfield, R. B., Gardner, E. P., and Calvert, J. G.: Sources and Sinks of Acetone in the Troposphere Behavior of Reactive Hydrocarbons and a Stable Product, J. Geophys. Res., 92(D4), 4208–4216, 1987.

de Reus, M., Fischer, H., Arnold, F., de Gouw, J., Holzinger, R., Warneke, C, and Williams, J.: On the relationship between acetone and carbon monoxide in different air masses, Atmos. Chem. Phys., 3, 1709–1723, doi:10.5194/acp-3-1709-2003, 2003.

Dufour, G., Szopa, S., Hauglustaine, D. A., Boone, C. D., Rinsland, C. P., and Bernath, P. F.: The influence of biogenic emissions on upper-tropospheric methanol as revealed from space, Atmos. Chem. Phys., 7, 6119–6129, doi:10.5194/acp-7-6119-2007, 2007.

Emmons, L. K., Hauglustaine, D. A., Muller, J. F., Carroll, M. A., Brasseur, G. P., Brunner, D., Staehelin, J., Thouret, V. and Marenco, A.: Data composites of airborne observations of tropospheric ozone and its precursors, J. Geophys. Res.-Atmos., 105, 20497–20538, 2000.

Emmons, L. K., Walters, S., Hess, P. G., Lamarque, J.-F., Pfister, G. G., Fillmore, D., Granier, C., Guenther, A., Kinnison, D., Laepple, T., Orlando, J., Tie, X., Tyndall, G., Wiedinmyer, C., Baughcum, S. L., and Kloster, S.: Description and evaluation of the Model for Ozone and Related chemical Tracers, version 4 (MOZART-4), Geosci. Model Dev., 3, 43–67, doi:10.5194/gmd-3-43-2010, 2010.

Fiore, A. M., Dentener, F. J., Wild, O., Cuvelier, C., Schultz, M. G., Hess, P., Textor, C., Schulz, M., Doherty, R., Horowitz, L. W., MacKenzie, I. A., Sanderson, M. G., Shindell, D. T., Stevenson, D. S., Szopa, S., Van Dingenen, R., Zeng, G., Atherton, C., Bergmann, D., Bey, I., Carmichael, G., Duncan, B. N., Faluvegi, G., Folberth, G., Gauss, M., Gong, S., Hauglustaine, D., Holloway, T., Isaksen, I. S. A., Jacob, D. J., Jonson, J. E., Kaminski, J. W., Keating, T. J., Lupu, A., Marmer, E., Montanaro, V., Park, R., Pitari, G., Pringle, K. J., Pyle, J. A., Schroeder, S., Vivanco, M. G., Wind, P., Wojcik, G., Wu, S., and Zuber, A.: Multi-model Estimates of Intercontinental Source-Receptor Relationships for Ozone Pollution, J. Geophys. Res., 114, D04301, doi:10.1029/2008JD010816, 2009.

Folberth, G. A., Hauglustaine, D. A., Lathière, J., and Brocheton, F.: Interactive chemistry in

ACPD
11, 9165–9215, 2011

the Laboratoire de Mtorologie Dynamique general circulation model: model description and impact analysis of biogenic hydrocarbons on tropospheric chemistry, Atmos. Chem. Phys., 6, 2273–2319, doi:10.5194/acp-6-2273-2006, 2006.

Hauglustaine, D. A., Hourdin, F., Jourdain, L. Filiberti, M.-A., Walters, S., Lamarque, J.-F., and Holland, E. A.: Interactive chemistry in the Laboratoire de Météorologie Dynamique general circulation model: Description and background tropospheric chemistry evaluation, J. Geophys. Res., 109, D04314, doi:10.1029/2003JD003957, 2004.

Hourdin, F., Musat, I., Bony, S., Braconnot, P., Codron, F., Dufresne, J.-L., Fairhead, L., Filiberti, M.-A., Friedlingstein, P., Grandpeix, J.-Y., Krinner, G., LeVan, P., Li, Z.-X., and Lott, F.: The LMDZ4 general circulation model: climate performance and sensitivity to parametrized physics with emphasis on tropical convection, Climate Dynamics, 19(15), 3445–3482, doi:10.1007/s00382-006-0158-0, 2006.

Jacob, D., Field, B., Jin, E., Bey, I., Li, Q., Logan, J., and Yantosca, R.: Atmospheric budget of acetone, J. Geophys. Res., 107, 4100, doi:10.1029/2001JD000694, 2002.

Krinner, G., Viovy, N., De Noblet-Ducoudré, N., Ogee, J., Polcher, J., Friedlingstein, P., Ciais, P., Sitch, A., and Prentice, I.: A dynamical global vegetation model for studies of the coupled atmosphere-biosphere system, Global Biogeochem. Cy., 19, GB1015, doi:10.1029/2003GB002199, 2005.

Köppe, M., Hermann, M., Brenninkmeijer, C. A. M., Heintzenberg, J., Schlager, H., Schuck, T., Slemr, F., Sprung, D., van Velthoven, P. F. J., Wiedensohler, A., Zahn, A., and Ziereis, H.: Origin of aerosol particles in the mid-latitude and subtropical upper troposphere and lowermost stratosphere from cluster analysis of CARIBIC data, Atmos. Chem. Phys., 9, 8413–8430, doi:10.5194/acp-9-8413-2009, 2009.

Lai, S. C., Baker, A. K., Schuck, T. J., van Velthoven, P., Oram, D. E., Zahn, A., Hermann, M., Weigelt, A., Slemr, F., Brenninkmeijer, C. A. M., and Ziereis, H.: Pollution events observed during CARIBIC flights in the upper troposphere between South China and the Philippines, Atmos. Chem. Phys., 10, 1649–1660, doi:10.5194/acp-10-1649-2010, 2010.

Lathière, J., Hauglustaine, D. A., Friend, A. D., De Noblet-Ducoudré, N., Viovy, N., and Folberth, G. A.: Impact of climate variability and land use changes on global biogenic volatile organic compound emissions, Atmos. Chem. Phys., 6, 2129–2146, doi:10.5194/acp-6-2129-2006, 2006.

Machida, T., Matsueda, H., Sawa, Y., Nakagawa, Y., Hirotani, K., Kondo, N., Goto, K., Nakazawa, T., Ishikawa, K., and Ogawa, T.: Worldwide measurements of atmospheric CO2

ACPD
11, 9165–9215, 2011

and other trace gas species using commercial airlines, J. Atmos. Oceanic. Technol., 25(10), 1744–1754, doi:10.1175/2008JTECHA1082.1, 2008.
Marandino, C. A., De Bruyn, W. J., Miller, S. D., Prather, M. J., and Saltzman, E. S.: Correction to "Oceanic uptake and the global atmospheric acetone budget", Geophys. Res. Lett., 33, L24801, doi:10.1029/2006GL028225, 2006.
Marenco, A., Thouret, V., Nedelec, P., Smit, H., Helten, M., Kley, D., Karcher, F., Simon, P., Law, K., Pyle, J., Poschmann, G., von Wrede, R., Hume, C., and Cook, T.: Measurement of ozone and water vapor by Airbus in-service aircraft: The MOZAIC airborne program, an overview, J. Geophys. Res., 103, 25631–25642, 1998.
Moore, D. P., Remedios, J. J., and Waterfall, A. M.: Global distributions of acetone in the upper troposphere from MIPASE spectra, Atmos. Chem. Phys. Discuss., 10, 23539–23557, doi:10.5194/acpd-10-23539-2010, 2010.
Olivier, J., Bouwman, A., van der Maas, C., Berdowski, J., Veldt, C., Bloos, J., Visschedijk, A., Zandveld, P., and Haverlag, J.: Description of edgar version 2.0: A set of global emission inventories of greenhouse gases and ozone-depleting substances for all anthropogenic and most natural sources on a per country basis and on a 1x1 degree grid, RIVM report 771060 002/TNO-MEP report R96/119, National Institute of Public Health and the Environment, 1996.
Olivier, J. and Berdowski, J.: Global emission sources and sinks, in: The Climate System, edited by: Berdowski, J., Guicherit, R., and Heij, B., A. A. Balkema Publishers/Swets & Zeitlinger Publishers, Lisse, 33–78, 2001.
Park, M., Randel, W. J., Kinnison, D. E., Garcia, R. R., and Choi, W.: Seasonal variation of methane, water vapor, and nitrogen oxides near the tropopause: Satellite observations and model simulations, J. Geophys. Res., 109, D03302, doi:10.1029/2003JD003706, 2004.
Potter, C., Klooster, S., Bubenheim, D., Singh, H. B., and Myneni, R., Modeling terrestrial biogenic sources of oxygenated organic emissions, Earth Interaction, 7, 1–15, 2003.
Pozzer, A., Pollmann, J., Taraborrelli, D., Jöckel, P., Helmig, D., Tans, P., Hueber, J., and Lelieveld, J.: Observed and simulated global distribution and budget of atmospheric C_2-C_5 alkanes, Atmos. Chem. Phys., 10, 4403–4422, doi:10.5194/acp-10-4403-2010, 2010.
Sanderson, M. G., Dentener, F. J., Fiore, A. M., Cuvelier, C., Keating, T. J., Zuber, A., Atherton, C. S., Bergmann, D. J., Diehl, T., Doherty, R. M., Duncan, B. N., Hess, P., Horowitz, L. W., Jacob, D., Jonson, J.-E., Kaminski, J. W., Lupu, A., Mackenzie, I. A., Marmer, E., Montanaro, V., Park, R., Pitari, G., Prather, M. J., Pringle, K. J., Schroeder, S., Schultz, M. G., Shindell, D. T.,

ACPD
11, 9165–9215, 2011

Szopa, S., Wild, O., and Wind, P.: A multi-model study of the hemispheric transport and deposition of oxidised nitrogen, Geophys. Res. Lett., 35, L17815, doi:10.1029/2008GL035389, 2008.
Scheele, M., Siegmund, P., and Velthoven, P. V.: Sensitivity of trajectories to data resolution and its dependence on the starting point: In or outside a tropopause fold, Meteorological Applications, 3, 267–273, doi:10.1002/met.5060030308, 1996.
Scheeren, H. A., Lelieveld, J., Roelofs, G. J., Williams, J., Fischer, H., de Reus, M., de Gouw, J. A., Warneke, C., Holzinger, R., Schlager, H., Klüpfel, T., Bolder, M., van der Veen, C., and Lawrence, M.: The impact of monsoon outflow from India and Southeast Asia in the upper troposphere over the eastern Mediterranean, Atmos. Chem. Phys., 3, 1589–1608, doi:10.5194/acp-3-1589-2003, 2003.
Schuck, T. J., Brenninkmeijer, C. A. M., Baker, A. K., Slemr, F., von Velthoven, P. F. J., and Zahn, A.: Greenhouse gas relationships in the Indian summer monsoon plume measured by the CARIBIC passenger aircraft, Atmos. Chem. Phys., 10, 3965–3984, doi:10.5194/acp-10-3965-2010, 2010.
Singh, H. B., Kanakidou, M., Crutzen, P. J., and Jacob, D. J.: High concentrations and photochemical fate of oxygenated hydrocarbons in the global troposphere, Nature, 378, 50–54, 1995.
Singh, H. B., Chen, Y., Staudt, A. C., Jacob, D. J., Blake, D. R., Heikes, B. G., and Snow, J.; Evidence from the southern Pacific troposphere for large global abundances and sources of oxygenated organic compounds, Nature, 410, 1078–1081, 2001.
Singh, H. B., Salas, L. J., Chatfield, R. B., Czech, E., Fried, A., Walega, J. Evans, M. J., Field, B. D., Jacob, D. J., Blake, D., Heikes, B., Talbot, R., Sachse, G., Crawford, J. H., Avery, M. A., Sandholm, S., and Fuelberg, H.: Analysis of the atmospheric distribution, sources, and sinks of oxygenated volatile organic chemicals based on measurements over the Pacific during TRACE-P, J. Geophys. Res., 109, D15S07, doi:10.1029/2003JD003883, 2004.
Solberg, S., Dye, C., Schmidbauer, N., Herzog, A., and Gehrig, R.: Carbonyls and nonmethane hydrocarbons at rural European sites from the Mediterranean to the Arctic, J. Atmos. Chem., 25, 33–66, 1996.
Sprung, D. and Zahn, A.: Acetone in the upper troposphere/lowermost stratosphere measured by the CARIBIC passenger aircraft: Distribution, seasonal cycle, and variability, J. Geophys. Res., 115, D16301, doi:10.1029/2009JD012099, 2010.
Thouret, V., Cammas, J.-P., Sauvage, B., Athier, G., Zbinden, R., Nédélec, P., Simon, P., and

ACPD
11, 9165–9215, 2011

Karcher, F.: Tropopause referenced ozone climatology and inter-annual variability (1994–2003) from the MOZAIC programme, Atmos. Chem. Phys., 6, 1033–1051, doi:10.5194/acp-6-1033-2006, 2006.

van der Werf, G. R., Randerson, J. T., Giglio, L., Collatz, G. J., Kasibhatla, P. S., and Arellano Jr., A. F.: Interannual variability in global biomass burning emissions from 1997 to 2004, Atmos. Chem. Phys., 6, 3423–3441, doi:10.5194/acp-6-3423-2006, 2006.

van Velthoven, P. F. J.: Meteorological analysis of CARIBIC by KNMI, available at: http://www.knmi.nl/samenw/campaign_support/CARIBIC/#LH, 2009.

Wennberg, P. O., Hanisco, T. F., Jaeglé, L., Jacob, D. J., Hintsa, E. J., Lanzendorf, E. J., Anderson, J. G., Gao, R. S., Keim, E. R., Donnelly, S. G., Del Negro, L. A., Fahey, D. W., McKeen, S. A., Salawitch, R. J., Webster, C. R., May, R. D., Herman, R. L., Proffitt, M. H., Margitan, J. J., Atlas, E. L., Schauffler, S. M., Flocke, F., McElroy, C. T., and Bui, T. P.: Hydrogen radicals, nitrogen radicals, and the production of ozone in the middle and upper troposphere, Science, 279, 49–53, 1998.

Xiong, X., Houweling, S., Wei, J., Maddy, E., Sun, F., and Barnet, C.: Methane plume over south Asia during the monsoon season: satellite observation and model simulation, Atmos. Chem. Phys., 9, 783–794, doi:10.5194/acp-9-783-2009, 2009.

ACPD
11, 9165–9215, 2011

Table 1. LMDz-INCA computation of acetone global budget terms, as well as literature results. Sources correspond to primary emission and chemical production, sinks correspond to deposition and chemical destruction. Primary emission and deposition are detailed according to continental/oceanic contributions.

Model		IMAGES Emmons et al. (2000)	GEOS-CHEM a posteriori Jacob et al. (2002)	Singh et al. (2004)	Marandino et al. (2006)	TOMCAT Arnold et al. (2005)	LMDz-INCA Folberth et al. (2006)	LMDz-INCA (this work)
Global atmospheric burden (Tg)			3.8		3.9	4.1		7.2
Residence time (days)			15	15	13	35		21
Source/sink strength (Tg acetone/year)			95	95	111	42.5		127
Primary emissions	Total	40	67	67		27	80	100
	Biogenic: terrestrial vegetation + plant decay		35	56			56	76
	Biomass burning		4.5	9			3.2	2.4
	Ocean		27	0		0	20	20
Chemical production	Total		28			15.5		27
Deposition	Total		23			9		47
	Oceanic deposition		14		62	0		28
	Land deposition		9		9			19
Chemical destruction	Total		73			33		80

ACPD
11, 9165–9215, 2011

Table 2. Statistics on the 11 geographical zones. Average and standard deviation are computed for all 2006 and 2007 flight sections included between minimum and maximum longitude and latitude, exclusively in the troposphere, for co-located modelling results and observation. Number of flights crossing the geographical zones is also given for each year. Computations are similarly made for whole flight, independently the location. Coordinates are also given for the two extended geographical regions Europe and South Asia, where budget terms are computed in Sect. 2. Focus regions are showed in bolt police.

Geographical zones	[min; max latitude] (°)	[min; max longitude] (°)	Number of flights crossing the region in 2006/2007	Observed mean± standard deviation (pptv) in 2006/2007	Simulated mean± standard deviation (pptv) in 2006/2007
Mid Latitude South America	[−35; −23.5]	[−72; −46]	4/0	380±235/*x*	870±840/*x*
Eastern South America	[−23.5; 0]	[−48; −20]	4/0	430±130/*x*	1090±540/*x*
Tropical Atlantic Ocean	[0; 24]	[−45; −10]	4/0	410±125/*x*	1150±580/*x*
North Atlantic Ocean (NAO)	[24; 60]	[−55; −10]	3/3	360±120/750±170	445±55/610±80
Eastern North America	[25; 60]	[−100; -55]	0/4	*x*/775±320	*x*/530±80
Europe-Mediterranean (EurMed)	**[30; 51]**	**[−10; 40]**	**9/9**	**775±520/865±500**	**710±170/695±100**
Northern Europe	[51; 60]	[−10; 40]	7/9	580±260/430±225	640±125/480±105
Northern Asia	[50; 60]	[40; 90]	4/8	720±280/655±380	700±50/595±215
Central Asia (CAs)	[30; 50]	[40; 90]	14/13	570±290/640±305	595±160/550±180
Central-South China (CSChi)	**[20; 40]**	**[90; 113]**	**15/16**	**610±305/585±270**	**790±305/690±310**
South China Sea (SCSea)	**[14; 25]**	**[113; 125]**	**14/14**	**445±180/450±240**	**695±235/620±190**
Whole flight	[−35; 60]	[−100; 125]	37/34	530±290/640±340	755±430/610±220
extended Europe	[30; 70]	[−10; 50]			
extended South Asia	[10; 40]	[50; 130]			

ACPD
11, 9165–9215, 2011

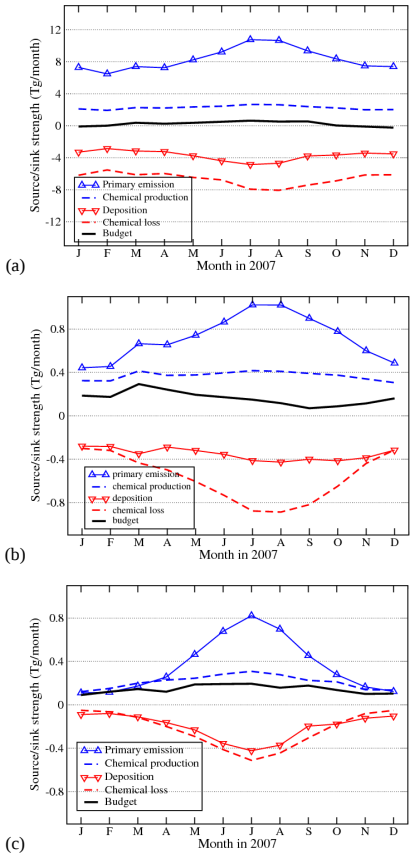

Fig. 1. Annual cycle of the acetone budget terms (in Tg month^{-1}), computed by LMDz-INCA for **(a)** the world, **(b)** South Asia, and **(c)** Europe. The net budget is computed as source – sink. Sources are divided into primary emission, and chemical production, and sinks (counted negatively) into dry deposition and chemical loss.

ACPD
11, 9165–9215, 2011

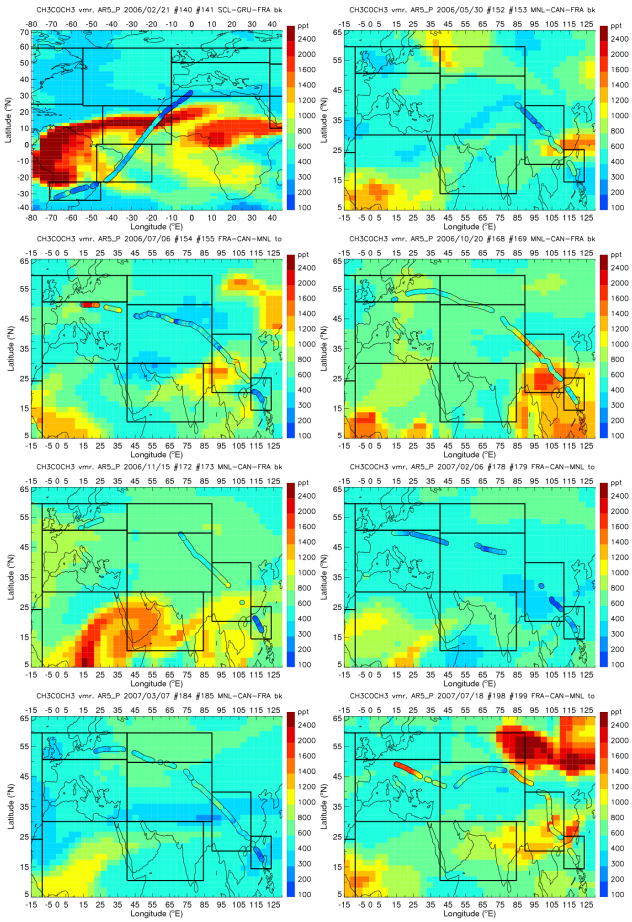

Fig. 2. Acetone vmr (pptv) acquired onboard the passenger aircraft along the flight trajectory for several flights, super imposed to maps of daily average of simulated acetone vmr at 238 hPa.

ACPD
11, 9165–9215, 2011

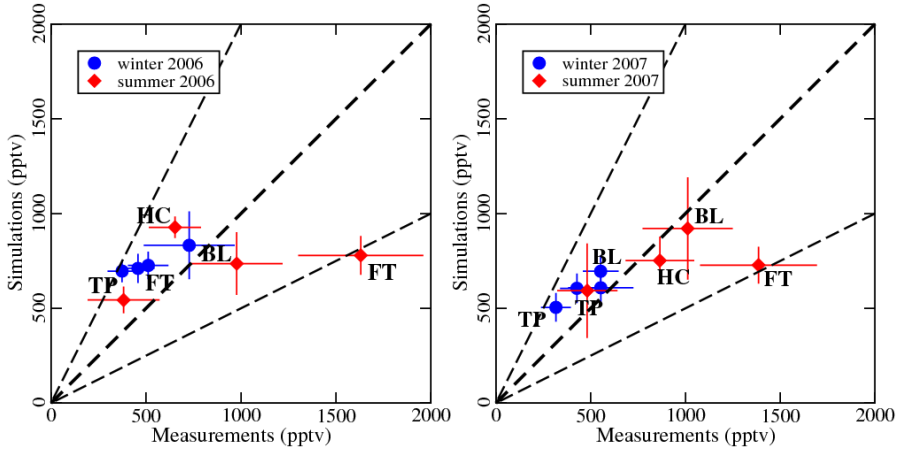

Fig. 3. Relation between simulated and measured acetone vmr (pptv) for flights of 2006 and 2007 to Manila. Annual averages are derived from co located simulations and airborne acquisition, making distinction according to the air mass print defined by Köppe et al. (2009), as FT for Free Troposphere, BL for Boundary Layer, HC for High Clouds and TP for tropopause. In winter 2007, dots not identified correspond to FT air mass print. Vertical and horizontal bars depict the standard deviation of acetone simulated and measured, respectively. Super imposed are three lines showing agreement ($x = y$), and a factor 2 difference between simulation and measurement ($y = 2x$ and $y = x/2$).

ACPD
11, 9165–9215, 2011

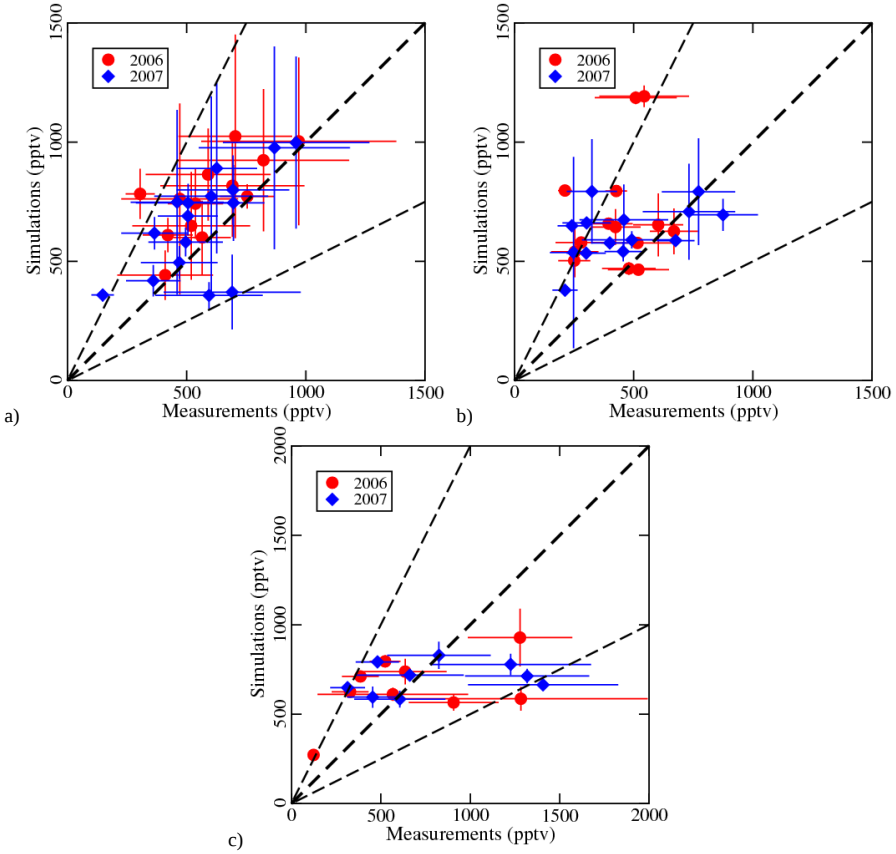

Fig. 4. As Fig. 3 except no distinction is made with air mass print but with geography and flight averages are plotted instead of seasonal averages: **(a)** Central-South China, **(b)** China Sea, and **(c)** Europe-Mediterranean region.

ACPD
11, 9165–9215, 2011

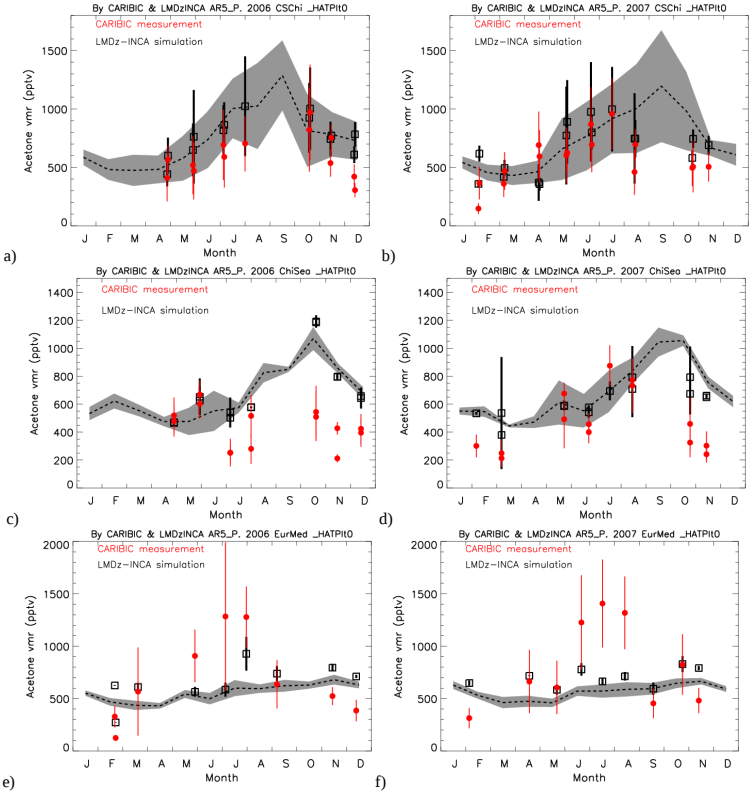

Fig. 5. Annual cycle of acetone vmr (pptv) simulated and measured in 7 months of 2006 and in 9 months of 2007 in UT over Central-South China (**a** and **b**) and South China Sea (**c** and **d**), and in 8 and 9 months of 2006 and 2007 respectively, over Europe-Mediterranean (**e** and **f**). Black empty squares and red filled circles present simulated and measured averages, respectively, with vertical bars for standard deviation. Intermittent line and shaded area present the climatological annual cycle: zone average of monthly simulations, and its standard deviation.

ACPD
11, 9165–9215, 2011

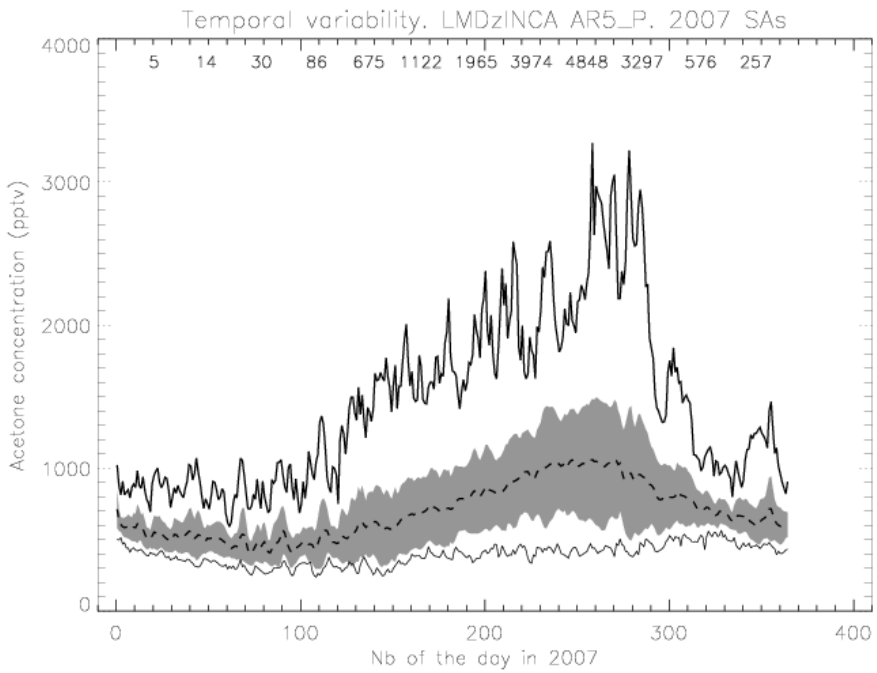

Fig. 6. Temporal and horizontal variability of acetone vmr (pptv) at 238 hPa over South Asia. Daily averages are provided by LMDz-INCA. Dashed line presents the region average, with the shaded zone for ±1 standard deviation. Full lines show spatial minimum and maximum acetone vmr for each day. Monthly number of values larger than 1000 pptv is indicated at the top of the Figure.

ACPD
11, 9165–9215, 2011

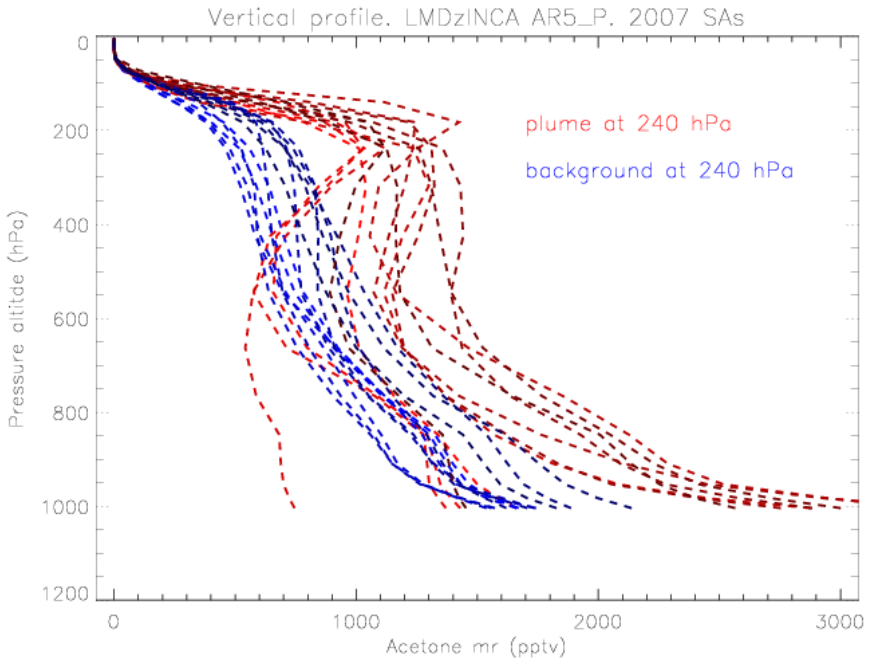

Fig. 7. Vertical profile of monthly average of acetone vmr simulated by LMDz-INCA over South Asia extended region, in background conditions and during 238-hPa ppbv-event (238-hPa acetone vmr >1000 pptv).

ACPD
11, 9165–9215, 2011

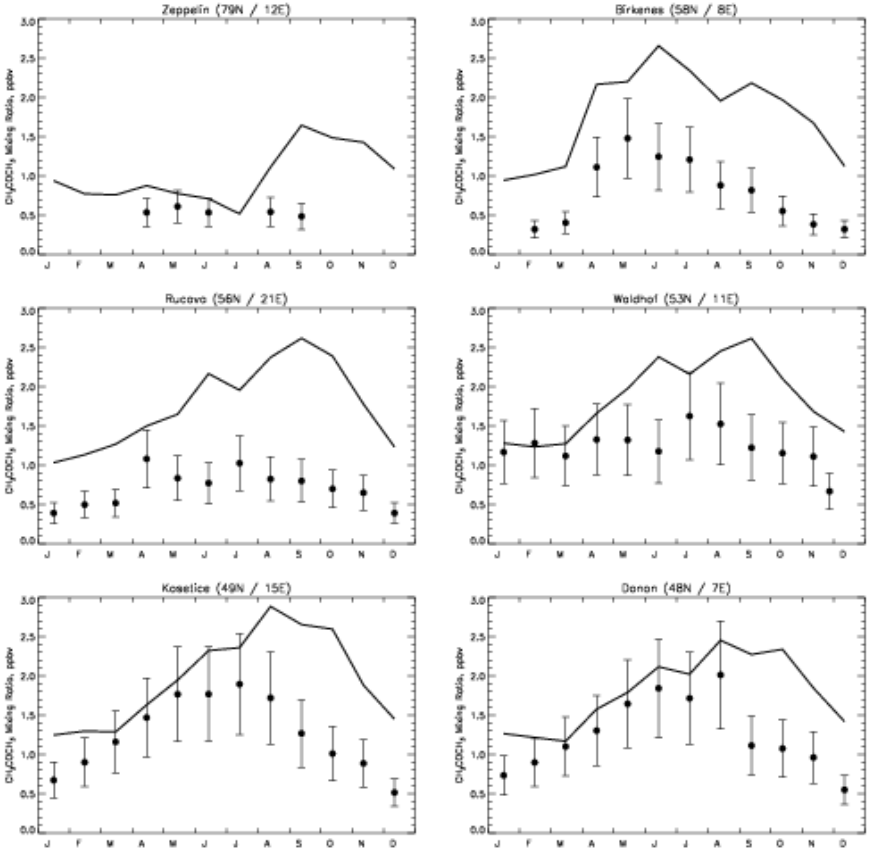

Fig. 8. Annual cycle of acetone vmr measured at surface level in 6 European stations (Solberg et al., 1996) (dots for averages and vertical bars for standard deviation), and climatological annual cycle computed by LMDz-INCA (line).

ACPD
11, 9165–9215, 2011

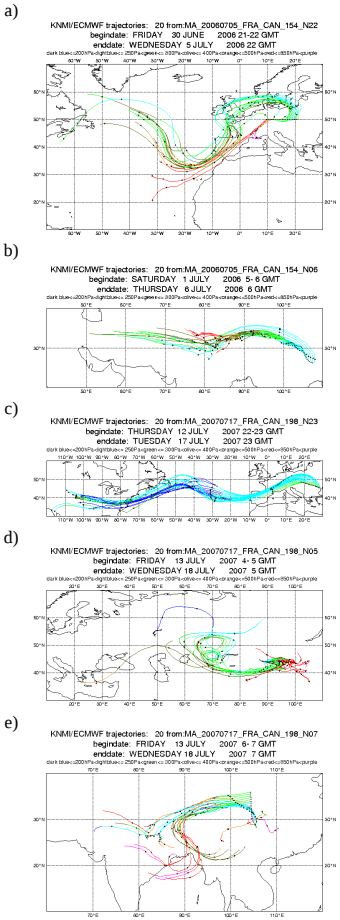

Fig. 9. KNLMI/ECMWF 5-day air mass back-trajectories (van Velthoven, 2009). Coordinates and dates of arrival points correspond to plumes sampled along the #154 and #198 July flights (Fig. 2).

ACPD
11, 9165–9215, 2011

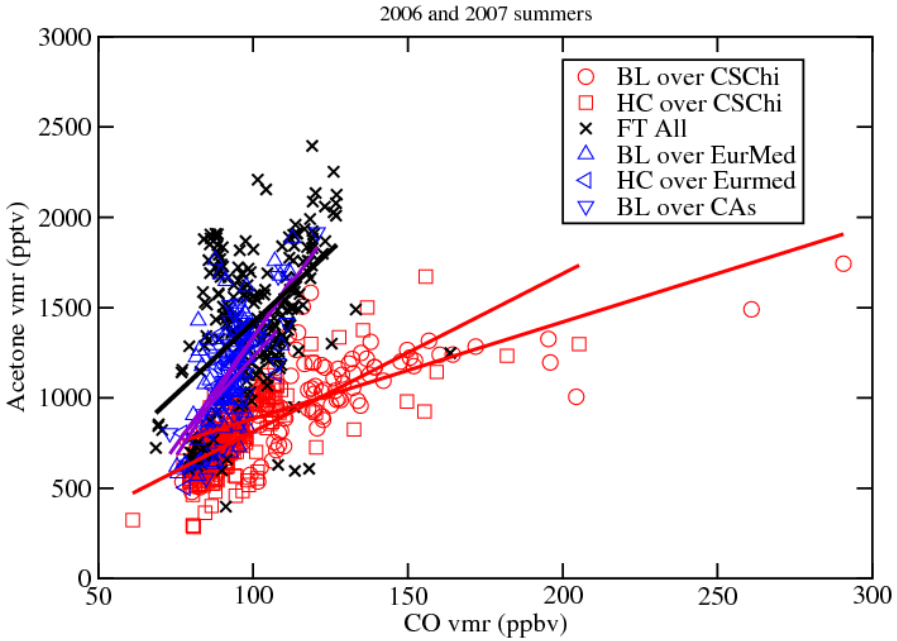

Fig. 10. Acetone/CO signature in various air masses sampled in 2006 and 2007 summers. Linear regressions are plotted in red for HC and BL air masses sampled over CSChi, in purple for same air masses but sampled over EurMed and Central Asia (CAs) and in black for all FT air masses sampled everywhere.

ACPD
11, 9165–9215, 2011

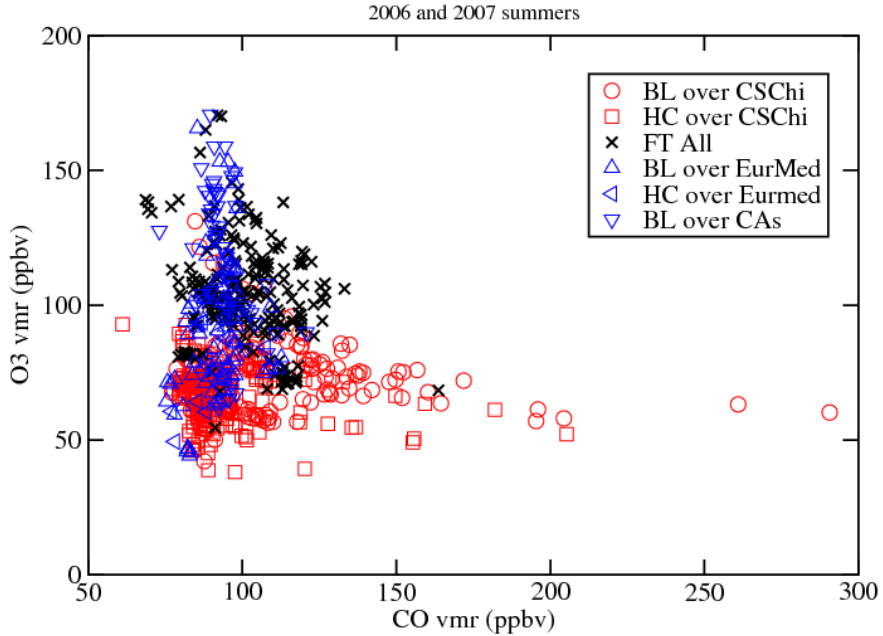

Fig. 11. O_3/CO signature of same air masses of Fig. 10, but as O_3 vmr plotted as a function of CO vmr.

ACPD
11, 9165–9215, 2011